Comparison of Piezoresistive and Capacitive Ultrasonic Transducers

John J. Neumann[a], David W. Greve[a] and Irving J. Oppenheim[b]

[a]Department of Electrical and Computer Engineering, Carnegie Mellon University, Pittsburgh, PA 15213;

[b]Department of Civil and Environmental Engineering, Carnegie Mellon University, Pittsburgh, PA 15213

ABSTRACT

MEMS ultrasonic transducers for flaw detection have heretofore been built as capacitive diaphragm-type devices. A diaphragm forms a moveable electrode, placed at a short gap from a stationary electrode, and diaphragm movement has been detected by capacitance change. Although several research teams have successfully demonstrated that technology, the detection of capacitance change is adversely affected by stray and parasitic capacitances, limiting the sensitivity of such transducers and typically requiring relatively large diaphragm areas. We describe the design and fabrication of what to our knowledge is the first CMOS-MEMS ultrasonic phased array transducer using piezoresistive strain sensing. Piezoresistors have been patterned within the diaphragms, and diaphragm movement creates bending strain which is detected by a bridge circuit, for which conductor losses will be less significant. The prospective advantage of such piezoresistive transducers is that sufficient sensitivity may be achieved with very small diaphragms. We compare transducer response under fluid-coupled ultrasonic excitation and report the experimental gauge factor for the piezoresistors. We also discuss the phased array performance of the transducer in sensing the direction of an incoming wave.

Keywords: Capacitive, diaphragm, MEMS, piezoresistive, ultrasonics

1. INTRODUCTION

Capacitive MEMS ultrasonic transducers (sometimes termed cMUTs, for capacitive MEMS Ultrasonic Transducers), have been studied by several research groups[1–6] both for liquid immersion applications[1–4] and also in contact with solid media.[5,6] In many of these applications fragility of the transducers is an important issue, so we developed a method of packaging the chips in silicone gel.[7] This will be shown here to be effective for packaging of CMOS-MEMS chips, which include a polysilicon layer that can easily be used for piezoresistive sensing. Resistive sensing has the advantage that it is not sensitive to parasitic capacitances, and thus can be used in small sizes and at longer distances of cabling. Here we present a comparison of capacitive and piezoresistive sensors packaged in silicone gels on DIPs (dual in-line packages).

2. TRANSDUCER FABRICATION

2.1. MUMPS Capacitive Transducers

The capacitive transducers used in this work were fabricated[7] using the MUMPS multi-user MEMS process on 1 cm^2 chips using the POLY0 and POLY1 layers. Each transducer consists of an array of hexagonal units and the upper electrode was released by etching the sacrificial SiO_2 layer through 5 μm square etch holes. An optical micrograph of one of the transducer arrays is shown in Fig. 1. This chip included a number of individual transducers, with variations in size, and design of diaphragm supports. For this paper, we used a transducer with a measured gap of 1.65 μm, and sensor capacitance of 12 pF. The various stray capacitances totaled 180 pF.

Further author information: (Send correspondence to J.J.N.)
J.J.N.: E-mail: jneumann@ece.cmu.edu, Telephone: 412 268 4404
D.W.G.: E-mail: dg07@andrew.cmu.edu, Telephone: 412 268 3707
I.J.O.: E-mail: ijo@cmu.edu, Telephone: 412 268 2950

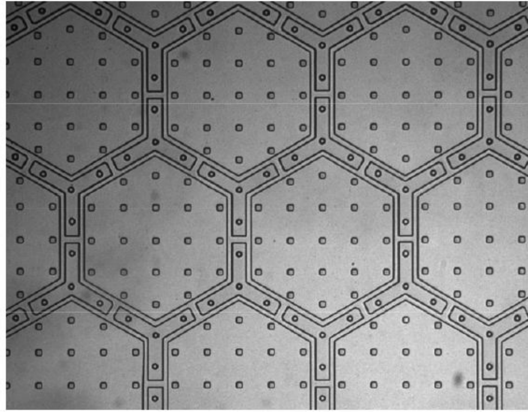

Figure 1. Photomicrograph of MUMPS capacitive sensor, showing several unit cells.

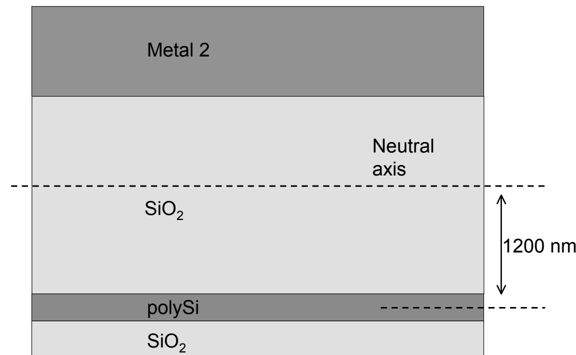

Figure 2. Cross section of beam showing thickness of metal and oxide layers, and location of polysilicon (which forms the piezoresistors).

2.2. CMOS Piezoresistive Transducers

Piezoresistive sensor chips were fabricated in the Agilent 0.5 μm process at MOSIS (www.mosis.org), and then processed using the CMOS-MEMS process developed at Carnegie Mellon.[8] A dry plasma of CHF_3 and O_2 was used to remove the overglass down to the silicon substrate, using any metal layers as a mask. Then a plasma of SF_6 was used to underetch the silicon, releasing the metal and oxide mechanical structures from the substrate. The CMOS polysilicon layer, which is towards the bottom of the beams (Figure 2), was used to create 16 resistive bridges, each with four 20 kilohm polysilicon resistors. Two of the resistors lie within a 95 by 170 μm rectangular diaphragm and are stressed when the diaphragm bends, and the other two lie under the solid areas of the chip and act as a reference (see Figure 3).

The diaphragms were formed of a grid of beams 2 μm wide and separated by 0.9 μm gaps. For uniform loading of a beam, we expect the greatest positive curvature in the middle and greatest negative curvature along the edges. We created two designs for our sensor, wherein the sensing piezoresistors occupy either the middle ("**M** sensors") or the edge ("**E** sensors") of a diaphragm. Because of the opposite curvature (assuming clamped beams), we expect opposite polarity signals from the two types of sensors. The resistor bridges are connected

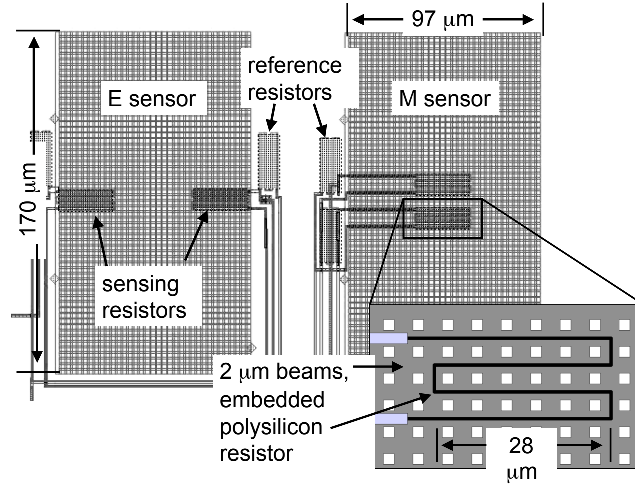

Figure 3. Layout of type **E** (left) and type **M** piezoresistive bridges on diaphragms. Crosshatch design is the diaphragm, and surrounding white area is solid (location of reference resistors).

to individual amplifiers on chip. Two sensors on each chip were directly wired to bond pads, so we were able to directly connect to the bridges using external circuitry, as discussed in Section 3.2.

3. EXPERIMENTAL SETUP

3.1. Packaging of the Devices

The capacitive sensors and the piezoresistive sensors were packaged in a similar way. The chips were mounted to dual in-line packages (DIPs) with silver epoxy (CW2400 from Circuitworks) and then baked for 30 minutes at 125 ^{o}C to ensure a full cure. After wire bonding, a silicone gel was applied by pouring while still in the liquid phase. For the capacitive sensor, we used Gelest Zipcone CG , a moisture-cured silicone gel, and for the piezoresistive sensor we used DOW Corning Sylgard 184, a two part PDMS gel. Before applying the Sylgard, the mixture was placed in a vacuum to remove air bubbles. In both cases, the silicone gel was applied by pouring slowly into a corner of the DIP cavity so that the bond wires were just covered. The surface tension of the silicone is great enough that the etch release holes (as large as 5 μm on the capacitive sensor) are sealed without the fluid dripping through. The silicone thickness in both cases was measured optically by measuring the height difference between the sensor chip and an ink spot on the surface of the transparent gel, taking into account the index of refraction of the material, around 1.4. The thickness of the gel over the piezoresistive sensor was between 500 and 600 μm. The thickness of the gel over the capacitive sensor varied from 400 to 700 μm over the size of the 1 cm chip. To hold water above the chip, plastic weighing dishes were glued to the top surface of the DIP packages with cyanoacrylate glue and then the seam was sealed with epoxy. The DIP package was inserted into a protoboard for electrical testing.

3.2. Measurement

The sensors were characterized by applying an external ultrasonic signal from a Krautkramer PZT transducer. The bottom of the transducer was partially submerged in the water, approximately 16 mm above the sensor. Pulses were supplied to the transducer from special hardware and software supplied by Krautkramer (Krautkramer MSW-QC, 5 MHz transducer, and Krautkramer USPC-2100 pulser/display unit). Signals were captured with a two channel oscilloscope and LabView software. One channel was attached, via a 100-to-1 resistive divider, to the Krautkramer transducer's driving voltage and acted as a trigger for the scope capture.

The MEMS sensor was connected directly to the other channel. The signal received on this channel was a combination of the signal of interest from the sensor with the electrical pickup of the high-voltage pulse which drove the Krautkramer transducer. Thus we could read off both the time of the pulse generation and the pulse arrival with the same scope trace. The scope was set to average either 8x, 64x, or 256x, as mentioned in the figure captions.

For the measurements on the capacitive sensor, a 10 volt DC voltage was applied to the substrate side of the sensor as shown in Figure 4. The moving electrode of the capacitor was connected directly to the digitizing scope (input impedance 1 MΩ in parallel with 13 pF). The measured sensor capacitance, with corrections for parasitics, is 12 pF. The total parasitic capacitance of the protoboard and cable used to connect to the scope is 180 pF. The DC voltage of 10 volts was chosen to be large while avoiding snapdown or arcing, and is also suitable for the resistive sensor measurements. Two measurements with opposite polarity DC bias were taken and algebraically subtracted to provide a differential signal.

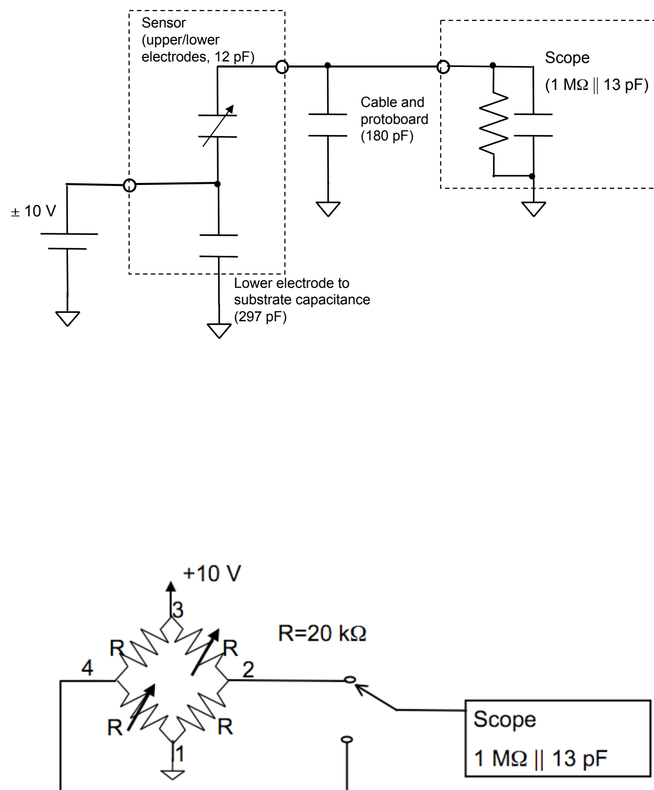

Figure 4. Measurement connections for capacitive and piezoresistive sensors.

For the measurements on the piezoresistive sensor, a DC voltage of 10 volts was applied across opposite corners of the bridge formed by the piezoresistors, as shown in Figure 4. The other two corners of the bridge (#2 and #4 in Figure 4) were individually measured, connected directly to the scope. The two signals were algebraically subtracted later to provide a differential signal.

The two diaphragms, one with an **E** sensor and one with an **M** sensor, have a center-to-center distance of 150 μm. To test the phased array behavior of the sensor chip, we captured waveforms from the two sensor elements while the source transducer was positioned several millimeters away from the sensors along the line passing through the sensor elements. These waveforms are discussed in section 4.2.

4. RESULTS

4.1. Single Sensor Behavior

The results of both piezoresistive and capacitive sensor measurements are shown in Figure 5. At the top is the voltage signal measured from the Krautkramer PZT source. This is a combination of the excitation pulse at $t = 5\mu$s, supplied by the pulsing setup, and a transduced pulse received by the source PZT around $t = 25\mu$s. This transduced pulse corresponds to a double path length reflection (travel from the source to the sensor surface and back), and allows us to estimate the distance as 16 mm. The distance is slightly different for the piezoresistive vs. the capacitive sensor (17 vs. 16 mm) because the measurement setup had to be moved to swap sensors.

In the case of the capacitive sensor, the waveform is the result of performing consecutive measurements with equal and opposite DC voltages (± 10 V) applied to the substrate, and then subtracting the measured waveforms to cancel the effect of the electromagnetic coupling to the source transducer (still visible at $t = 5\mu$s). In a similar manner, the piezoresistive sensor was measured at two points (nodes 2 and 4, which give opposite sense signals by design) and subtracted to give a differential signal, which is plotted in Figure 5.

The signal from each of the sensors appears as a series of approximately 1 μs pulses that die out, which is consistent with the arriving pulse undergoing multiple reflections between the water-silicone interface and the sensor chip with a sound speed of 0.8-1.4 mm/μs. We expect some reflections of the ultrasonic pulse between the MEMS and Krautkramer transducer, and also from the interface between the two different media (water and silicone gel). The characteristic acoustic impedance of water is 1.5x10^5 g/(cm^2·s); in previous work[7] we estimated the acoustic impedance of the silicone gel to be 2x10^5 g/(cm^2·s). The acoustic impedance (at 1 MHz) of the CMOS diaphragm was calculated (an upper limit based on a solid plate), based on known material properties, to be 4x10^4 g/(cm^2·s), about an order of magnitude less than the surrounding medium. The acoustic impedance of the MUMPS capacitive electrode plates is less than 1000 g/(cm^2·s).

4.2. Phased Array Behavior

Waveforms were captured from both sensor elements of the piezoresistive chip, while positioning the source transducer at opposite ends of the sensor chip. Detail views of the arriving pulses are shown in Figure 6, corrected for the polarity difference between the sensor elements. In the left hand graph, the source was on the side of the sensor chip closest to the **E** sensor element; we see the pulse arrival is about 0.1 μs earlier for the **E** sensor element than the **M** element, which is consistent with a 1.55 mm/μs sound speed in water and 150 μm element pitch. The opposite is true when the source is placed on the side of the chip closer to the **M** sensor element. The time delay is slightly smaller than expected, due to the angle of the source above the plane of the sensor chip, and a change in peak shape due to multiple-path reflections.

5. DISCUSSION

The area of one of the capacitive sensor elements is 2.24×10^6 μm^2; one of the piezoresistive elements, including the area around the diaphragm needed for the inactive resistors in the bridge, is 22,100 μm^2 (about 100 times smaller). The piezoresistive sensor is clearly superior in terms of signal for a given size. The noise level for the capacitive sensor element is also noticeably higher than the piezoresistive sensor, though we did not quantify it.

The waveform from the capacitive sensor is closer to a single pulse than the waveform from the piezoresistive sensor. This is probably due to the different boundary conditions encountered by the incoming wave. The

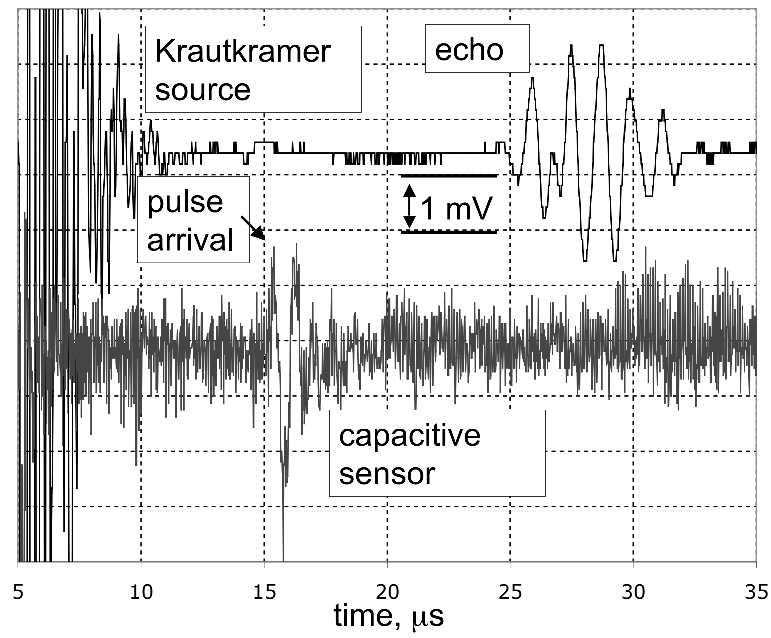

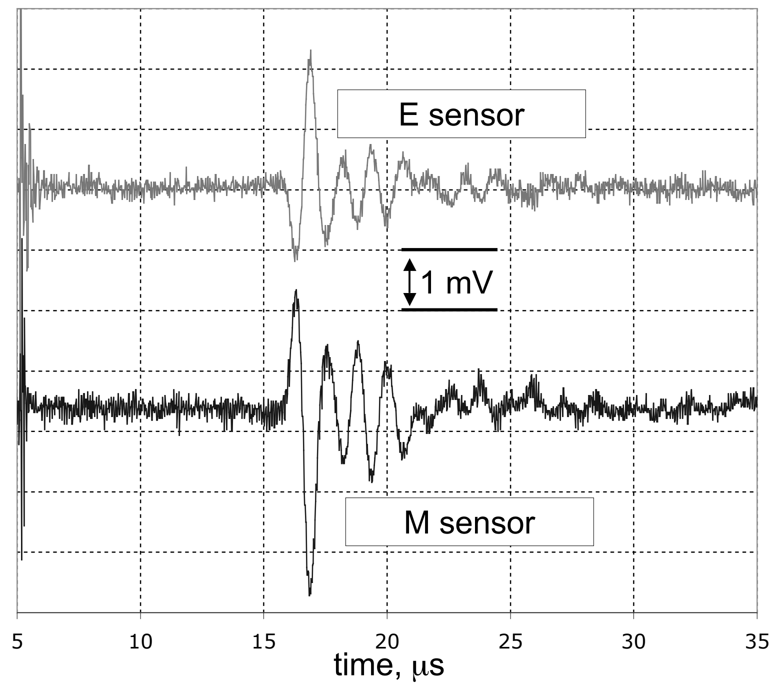

Figure 5. Waveforms (8x averaging) measured from piezoresistive and capacitive sensors, with source 16 mm from surface of sensor.

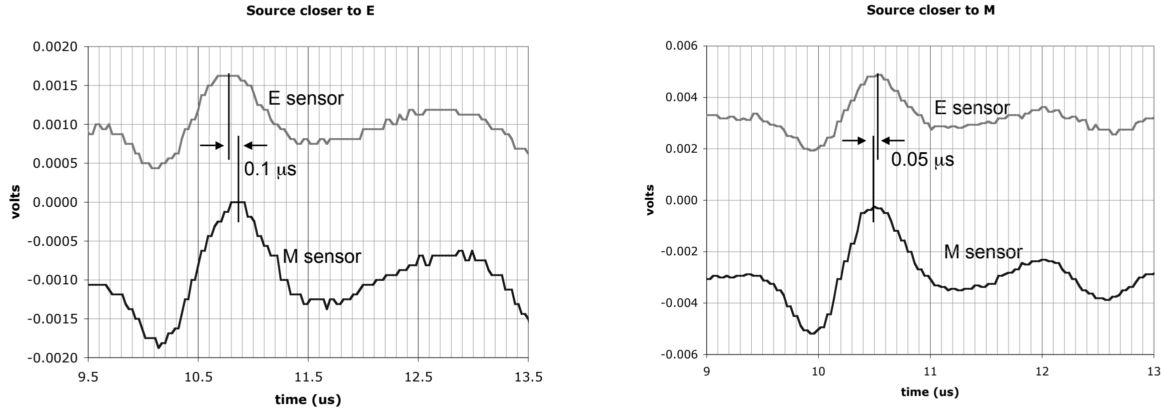

Figure 6. Pulse (256x averaging) arriving at slightly different times for the two sensor elements, for two different source positions.

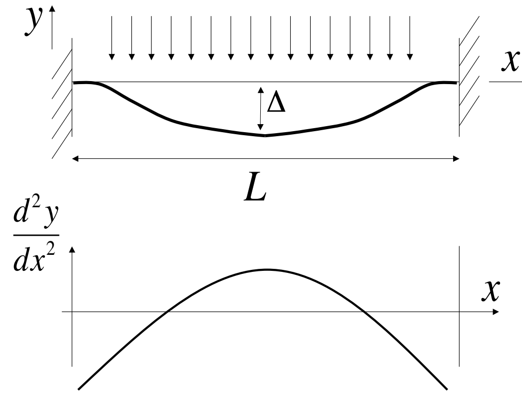

Figure 7. Drawing of beam deflection and strain.

capacitive sensor chip has a larger fraction (about half) of its area populated by sensors, lowering the acoustic impedance of the surface as a whole compared to the mostly solid CMOS chip with its much smaller diaphragms. Thus we expect different reflection patterns between the sensor surface and the water/gel interface.

We estimate the diaphragm deflection and the gauge factors of the piezoresistive sensors from a series of assumptions. We first assume that the capacitive and the piezoresistive diaphragms both move with the particle velocity (wave motion) of the silicone gel, because of the low acoustic impedance of the diaphragm structures. From the measured capacitance of the capacitive sensor, 12 pF, we calculate a gap dimension of 1.65 μm, and from the signal level obtained, and corrected for the total parasitic capacitance of 193 pF, we obtain an equivalent parallel-plate deflection of 2.1 nm. We approximate the hexagonal diaphragm of the capacitive sensor as a circular diaphragm with a clamped boundary, for which the average deflection is 29 % of that at the center, to obtain 7.3 nm for the deflection at the center of the capacitive diaphragm.

We then envision the piezoresistive diaphragm as a one-way plate, clamped along both edges, loaded by uniform downward pressure to a central deflection of 7.3 nm. Figure 7 shows the deflection and curvature in a

plate (or beam) with span length L and central deflection Δ. The curvature can be expressed as

$$\text{curvature} = \frac{d^2y}{dx^2} = \frac{-32\Delta}{L^2}\left[1 - 6\frac{x}{L} + 6\left(\frac{x}{L}\right)^2\right]. \tag{1}$$

The minimum curvature occurs at the edge and is equal to $-32\Delta/L^2$, and the maximum curvature occurs at the middle and is equal to $16\Delta/L^2$. In the piezoresistive diaphragm, the span length L is 97 μm and the sensor length (both **E** and **M**) is 28 μm. The average curvature over the length of the **E** sensor is $-9.6\Delta/L^2$, and the average curvature over the length of the **M** sensor is $14.6\Delta/L^2$. The signals from the **E** and **M** sensors in Figure 5 show the predicted opposition in sign.

At any location along the span the strain is obtained as the curvature multiplied by the distance (approximately 1.2 μm) from the neutral axis to the center of the piezoresistor. For the span length of 97 μm and the estimated deflection Δ of 7.3 nm, the average strains at the **E** and **M** sensors under a uniform downward pressure are estimated as -9 and 14 $\mu\epsilon$, respectively, where tensile strain is positive. Our loading is a pulse, and at the **E** sensor we initially see a 2 mV voltage decrease in the differential signal (a resistance increase, dR/R of 0.0004) followed by a voltage increase of roughly twice that amplitude; at the **M** sensor we initially see a 3.5 mV voltage increase (a resistance decrease, dR/R of -0.0007) followed by a voltage decrease of roughly twice that amplitude; we assume the initial arrival to correspond to the imposed central (downward) deflection of 7.3 nm, and we attribute the larger signal on the next half-cycle as a dynamic response of the membrane. The gauge factor may be defined as the ratio of dR/R to strain, and using the resistance changes associated with first arrival of the pulse, gauge factors of -45 and -51 are obtained at the **E** and **M** locations, respectively. While these are somewhat larger than values (-15 to -22) reported by other researchers[9, 10] for MEMS-based n-polysilicon material, they are close to each other, indicating our acoustic and mechanical assumptions are reasonable.

6. CONCLUSIONS

We conclude that piezoresistive MEMS sensors hold advantages in size and sensitivity over capacitive transducers. The size advantage stems from the fact that capacitive transducers' signal strength depends on sensor element area compared to parasitic capacitances in the measurement setup; resistive sensors are not subject to this limitation. The absolute magnitudes of resistances also depend in a different manner on size than do capacitances, so it is possible to build very small transducers. We foresee these tiny transducers being used for applications where unobtrusive placement is a consideration (flaw detection), and in array applications, e.g. medical imaging, as the sensor size is no longer an impediment to arbitrary positioning. The low output impedance (kilohms) of the piezoresistive sensor allows it to be used with longer cables and a greater variety of signal conditioning devices (amplifiers) without signal degradation.

CMOS-MEMS technology in particular is well suited for piezoresistive ultrasonic sensors. A polysilicon layer for making resistors is a part of most standard CMOS processes, and can easily be designed into mechanical structures which are sensed by on-chip amplification circuitry.

ACKNOWLEDGMENTS

This material is based upon work supported by the National Science Foundation under Grant No. CMS-0329880. Any opinions, findings, and conclusions or recommendations expressed in this material are those of the authors and do not necessarily reflect the views of the National Science Foundation. This work was also supported by the Commonwealth of Pennsylvania through the Pennsylvania Infrastructure Technology Alliance program, and DARPA's ASIMPS program. The authors would also like to acknowledge gifts from Krautkramer Inc.

REFERENCES

1. P.-C. Eccardt, K. Niederer, T. Scheiter, and C. Hierold, "Surface micromachined ultrasound transducers in CMOS technology," *1996 IEEE Ultrasonics Symposium*, pp. 959–962, 1996.
2. A. Bashford, D. Schindel, and D. Hutchiny, "Micromachined ultrasonic capacitance transducers for immersion applications," *IEEE Transactions on Ultrasonics, Ferroelectrics, and Frequency Control* **45**, pp. 367–375, 1998.

3. X. Jin, I. Ladabaum, F. Degertekin, S. Calmes, and B. Khuri-Yakub, "Characterization of one-dimensional capacitive micromachined ultrasonic immersion transducer arrays," *IEEE Journal of Microelectromechanical Systems* **8**, pp. 100–114, 1999.
4. X. Jin, O. Oralkan, F. Degertekin, and B. Khuri-Yakub, "Characterization of one-dimensional capacitive micromachined ultrasonic immersion transducer arrays," *IEEE Transactions on Ultrasonics, Ferroelectrics, and Frequency Control* **48**, pp. 750–760, 2001.
5. I. Oppenheim, A. Jain, and D. Greve, "MEMS ultrasonic transducers for the testing of solids," *IEEE Transactions on Ultrasonics, Ferroelectrics, and Frequency Control* **50**, pp. 305–311, 2003.
6. D. Greve, A. Jain, and I. Oppenheim, "MEMS phased array detection in contact with solids," in *2003 IEEE Ultrasonics Symposium*, IEEE, ed., pp. 5D–6, 2003.
7. D. Greve, J. Neumann, I. Oppenheim, S. Pessiki, and D. Ozevin, "Robust capacitive MEMS ultrasonics transducers for liquid immersion," in *2003 IEEE International Ultrasonics Symposium Oct 5-8, 2003 Honolulu, Hawaii conference of the Ultrasonics Ferroelectrics, and Frequency Control Society*, pp. 3F–4, 2003.
8. G. Fedder, S. Santhanam, M. Reed, S. Eagle, D. Guillou, M.-C. Lu, and L. Carley, "Laminated high-aspect-ratio microstructures in a conventional CMOS process," *Sensors and Actuators A* **57**, pp. 103–110, 1996.
9. L. Cao, T. S. Kim, J. Zhou, S. C. Mantell, and D. L. Polla, "Calibration technique for MEMS membrane type strain sensors," *Proc. Thirteenth Biennial University/Government/Industry IEEE Microelectronics Symposium*, pp. 204–210, 1999.
10. P. French and A. Evans, "Polycrystalline silicon strain sensors," *Sensors and Actuators* **8**, pp. 219–225, 1985.